

Supplementary Information

Importance of the Alignments of Polar π Conjugated Molecules inside Carbon Nanotubes in Determining Second-order Non-linear Optical Properties

Takashi Yumura* and Wataru Yamamoto

*Faculty of Materials Science and Engineering, Graduate School of Science and
Technology, Kyoto Institute of Technology, Matsugasaki, Sakyo-ku, Kyoto, 606-8585,
Japan*

- S1. **Origin of host-guest interactions in $1 \times \text{DANS}@ (m,m)$**
- S2. **Energetics of antiparallel linear DANS dimers with a function of the intermolecular separation**
- S3. **Intermolecular interactions in a stacking DANS dimer taken from $2 \times \text{DANS}@ (m,m)$**
- S4. **Structures for $3 \times \text{DANS}@ (10, 10)$**
- S5. **Shifting one DANS molecule from the original cofacial arrangement plays an important role in determining the intermolecular interactions.**
- S6. **Optimized geometries for DANS dimers inside a zigzag nanotube ($2 \times \text{DANS}@ (m,0)$)**

*To whom all correspondence should be addressed.
E-mail; yumura@kit.ac.jp

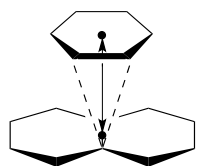
S1. Origin of host-guest interactions in $1 \times \text{DANS}@(\text{m},\text{m})$

Here let us discuss origin of host-guest interactions in $1 \times \text{DANS}@(\text{m},\text{m})$. For this purpose, methyl and benzene groups in DANS were modeled by methane and benzene, respectively, and six-membered rings in nanotubes are modeled by benzene or naphthalene. Then, we investigated the total energy changes of benzene approaching naphthalene with two fashions (Scheme S1a) as well as methane approaching benzene (Scheme S1b). In Scheme S1a, π - π interactions are operated between a C atom of naphthalene ($\text{C}(\text{C}_{10}\text{H}_8)$) and that of benzene $\text{C}(\text{C}_6\text{H}_6)$, and CH- π interactions are operated between a C atom of naphthalene ($\text{C}(\text{C}_{10}\text{H}_8)$) and an H atom of benzene $\text{H}(\text{C}_6\text{H}_6)$. Only, CH- π interactions are considered between an H atom of methane $\text{H}(\text{CH}_4)$ and a C atom of benzene ($\text{C}(\text{C}_6\text{H}_6)$) in Scheme S1b.

The potential energy surfaces along the three pathways were obtained by B97D calculations using the 6-31++G** basis set. Then, the total energies (E_{total}) of C_6H_6 - C_{10}H_8 and CH_4 - C_6H_6 systems relative to the dissociation limit to the two molecules are plotted in Fig. S1-1. Fig. S1-1 shows only one minimum exists in each PES, which are represented by the equilibrium separation (S_e) and the stabilization energy from the non-covalent interactions (E_{min}) (Table S1). For the CH $\cdots\pi$ interactions in the C_6H_6 - C_{10}H_8 and CH_4 - C_6H_6 complexes, the S_e values were computed to be 2.87 and 2.99 Å, respectively. Additionally, the B97-D calculations provided the S_e value of 3.65 Å for the π - π interactions in the C_6H_6 - C_{10}H_8 complex. The strength of no-bonding interactions, denoted by E_{min} , decreases in the order: CH- π interactions in the C_6H_6 - C_{10}H_8 complex (-4.6 kcal/mol) > π - π interactions in the C_6H_6 - C_{10}H_8

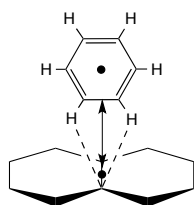
Scheme S1

(a) benzene approaching naphthalene

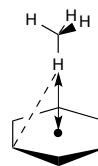


π - π interactions

(b) methane approaching benzene



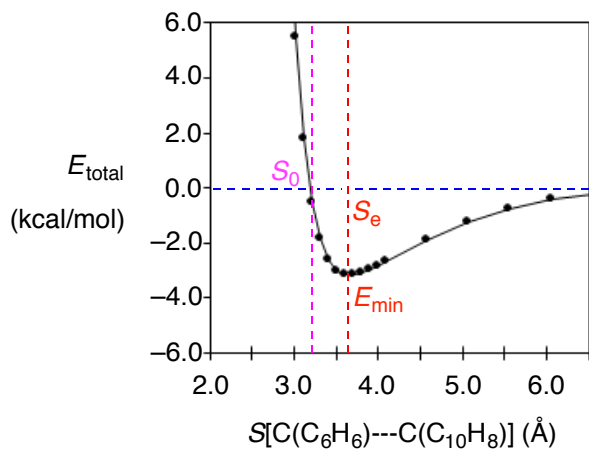
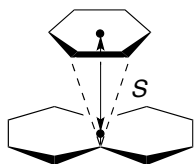
CH- π interactions



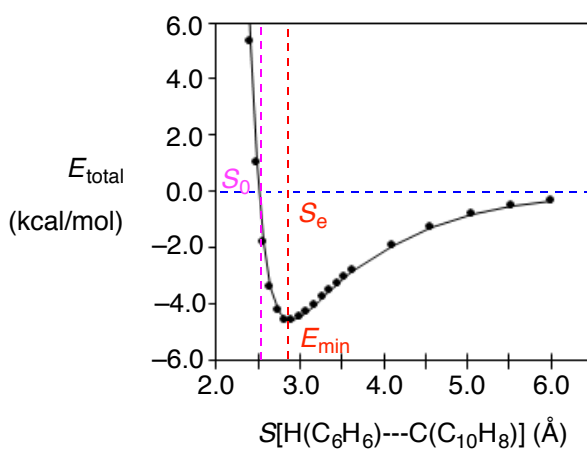
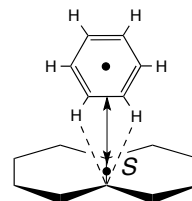
CH- π interactions

(a) benzene approaching naphthalene

(i) π - π interactions



(ii) CH- π interactions



(b) methane approaching benzene

(i) CH- π interactions

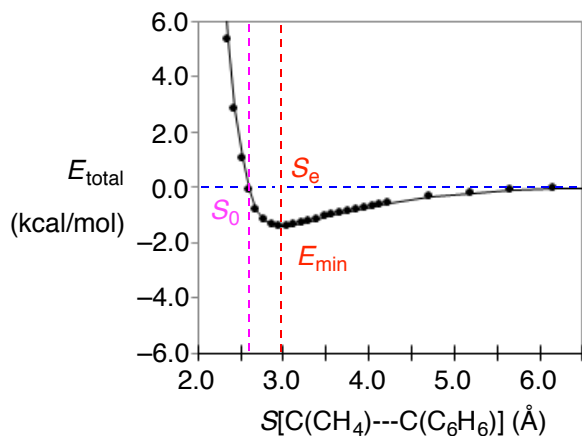
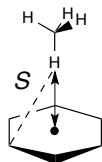


Fig. S1-1 The potential energy surface (PES) for (a) benzene approaching naphthalene, as well as (b) methane approaching benzene. The PES were obtained from the B97-D/6-31++G** calculations. The energy values relative to the dissociation limit toward benzene and naphthalene (methane and benzene) are given. In (a), we considered two types of interactions; (i) π - π and (ii) CH- π interactions, and in (b) (ii) CH- π interactions were only considered. Key parameters, S_e , E_{min} , and S_0 , defined in this figure, were listed in Table S1.

complex (-3.2 kcal/mol) > CH- π interactions in the CH₄-C₆H₆ complex (-1.4 kcal/mol). Table S1 also lists the intermolecular separation in the complexes whose E_{total} value is zero, denoted by S_0 . For the CH- π interactions, the S_0 values in the C₆H₆-C₁₀H₈ and CH₄-C₆H₆ complexes are 2.50 and 2.59 Å, respectively, and that in the C₆H₆-C₁₀H₈ complex is 3.19 Å for the π - π interactions

Considering the non-bonding interactions obtained from the small models, we assume that the weak CH- π and π - π interactions occur between the DANS guest and a tube host in the optimized $1 \times \text{DANS}@ (m,m)$ structures (Fig. 2). To verify this assumption, we investigated in $1 \times \text{DANS}@ (m,m)$ ($m = 6, 7,$ and 10) the distribution of the internuclear separation between the DANS guest and the nanotube host for distances ranging from 2.4 to 4.5 Å. Fig. S1-2 shows the number of 0.1 Å internuclear separations between the inner DANS and a nanotube per unit interval. For each $1 \times \text{DANS}@ (m,m)$ structure in Fig. S1-2, there are two histograms representing the separations of a C atom in DANS from a C atom in the tube (C(DANS)···C(tube)), and those of an H atom in DANS from a C atom of the tube (H(DANS)···C(tube)).

For the B97D optimized $1 \times \text{DANS}@ (7,7)$ structure, H atoms of the DANS guest separate from tube C atoms by a distance greater than 2.6 Å (Fig. S1-2b). Considering the potential energy surfaces shown in Figs. S1-1, this separation range indicates that the DANS guest is bound to the (7,7) nanotube by attractive CH··· π interactions. A substantial number of H(DANS)···C(tube) contacts was observed at approximately 2.9 Å, which corresponds to the equilibrium separation in the methane-benzene and benzene-naphthalene complexes. A similar observation was made for the

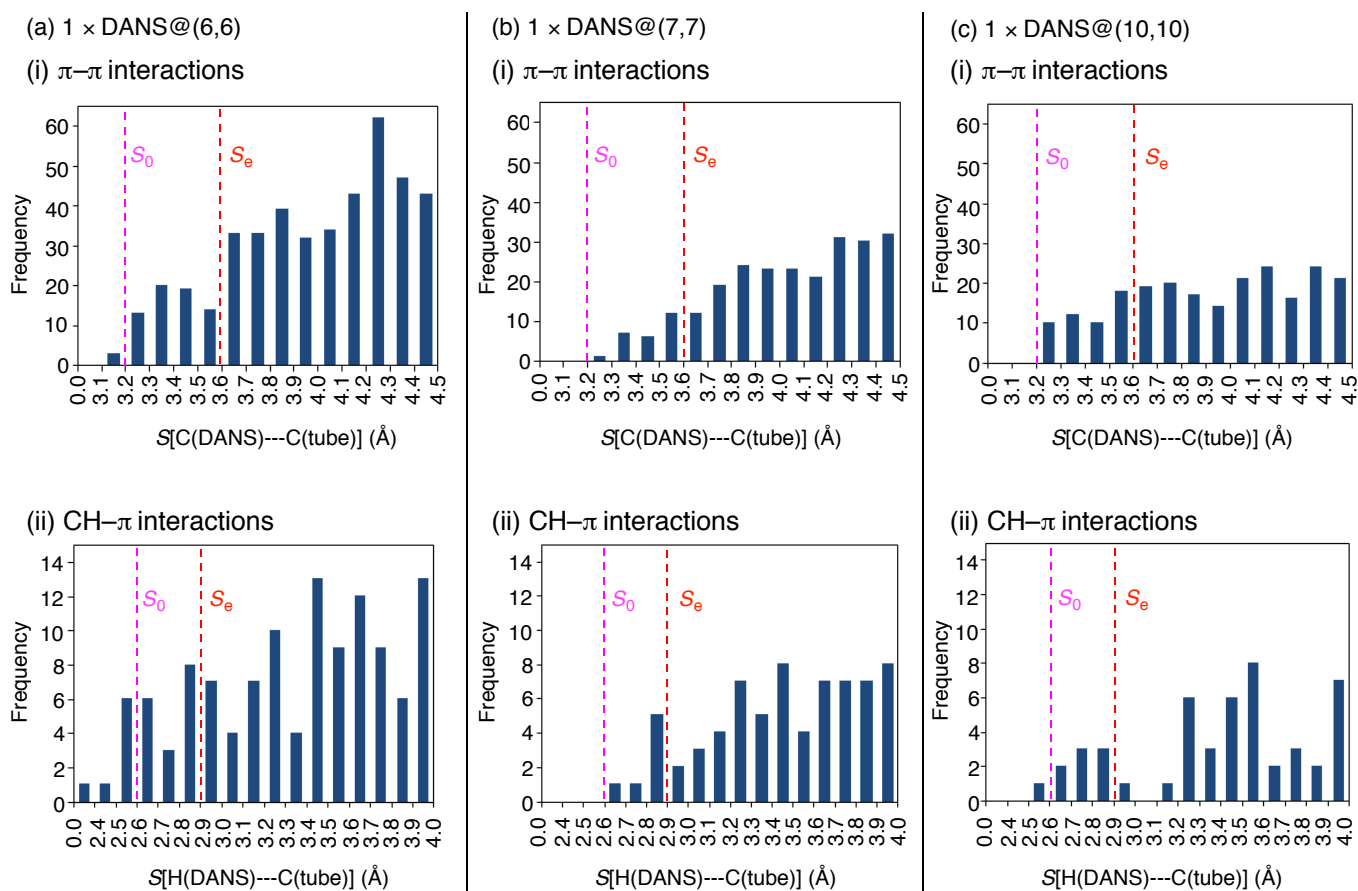


Fig. S1-2 Distribution of the internuclear separations between the DANS guest and the nanotube wall of (a) 1 xDANS@(6,6), (b) 1 xDANS@(7,7), and (c) 1 xDANS@(10,10). (i) separations between a C atom of the guest and a C atom of the host tube ($S[C(DANS)\cdots C(\text{tube})]$) and (ii) those between an H atom of the guest and a tube C atom ($S[H(DANS)\cdots C(\text{tube})]$). The key geometrical parameters (S_0 and S_e) in the π - π and CH- π interactions, obtained in Figure S1-1, are given by dotted lines.

$\pi\cdots\pi$ interactions in the $1 \times \text{DANS}@ (7,7)$ structure; larger number of $\text{C}(\text{DANS})\cdots\text{C}(\text{tube})$ contacts was observed at approximately 3.6 Å, which is equal to the S_e value in the benzene–naphthalene complex (Fig. S1-1). These analyses indicate that the DANS guest inside a nanotube is stabilized by both attractive $\text{CH}\cdots\pi$ and $\pi\cdots\pi$ interactions. Similar tendencies can be found in $1 \times \text{DANS}@ (10,10)$ in terms of operation of attractive $\text{CH}\cdots\pi$ and $\pi\cdots\pi$ interactions. Compared to the $1 \times \text{DANS}@ (7,7)$ structure, the number of $\text{H}(\text{DANS})\cdots\text{C}(\text{tube})$ and $\text{C}(\text{DANS})\cdots\text{C}(\text{tube})$ contacts over 2.6 and 3.2 Å, respectively, decreased in the $1 \times \text{DANS}@ (10,10)$ structures, explaining less significant E_{bind} value in $1 \times \text{DANS}@ (10,10)$ than the $1 \times \text{DANS}@ (7,7)$ case, as seen in Table 1.

In contrast to the $1 \times \text{DANS}@ (7,7)$ and $1 \times \text{DANS}@ (10,10)$ structures, state of affairs is little different in $1 \times \text{DANS}@ (6,6)$, where the host tube has a smaller diameter. In this situation, we found some numbers of $\text{H}(\text{DANS})\cdots\text{C}(\text{tube})$ and $\text{C}(\text{DANS})\cdots\text{C}(\text{tube})$ contacts below 2.6 and 3.2 Å, respectively, indicating operating repulsive $\text{CH}\cdots\pi$ and $\pi\cdots\pi$ interactions between the host and guest. Furthermore, deformation of a (6,6) tube induced by the encapsulation of DANS molecule costs the energy of 14.2 kcal/mol. As a result of operating the repulsive interactions due to too short contacts between the host and guest, as well as the destabilization induced by the tube deformation, less significant E_{bind} value in $1 \times \text{DANS}@ (6,6)$ is understandable. Accordingly, these statistical analyses can help to understand that E_{bind} values depend on host-tube diameters in Fig. 3.

Table S1 Key parameters in the potential energy surfaces of benzene approaching naphthalene with two orientations, as well as methane approaching benzene.

| Models | C ₆ H ₆ -C ₁₀ H ₈ complex | | CH ₄ -C ₆ H ₆ complex |
|--------------|---|------------------------|--|
| Interactions | π - π interactions | CH- π interactions | CH- π interactions |
| S_0 | 3.19 | 2.50 | 2.59 |
| S_e | 3.65 | 2.87 | 2.99 |
| E_{\min} | -3.2 | -4.6 | -1.4 |

S_0 (Å): Separation in the complexes are energetically identical to the dissociation limit toward the two molecules

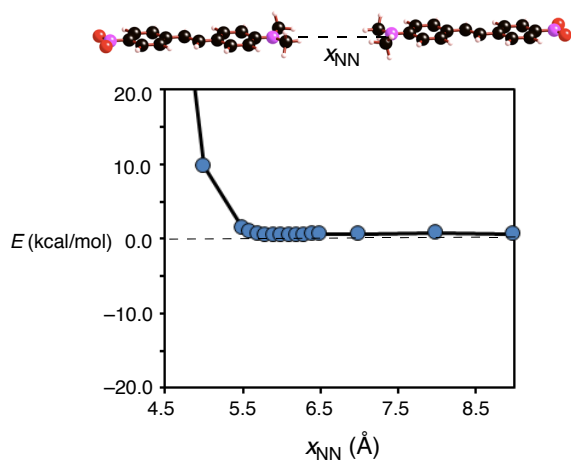
S_e (Å): Equilibrium separation in one local minimum on each PES.

E_{\min} (kcal/mol): Stabilization energy from the non-bonding interactions in the complexes.

S2. Energetics of antiparallel linear DANS dimers with a function of the intermolecular separation

We obtained potential energy surface of DANS dimers in antiparallel linear alignment with a function of x_{NN} defined in Fig. S2. Energetics of the DANS dimers relative to the dissociation limit toward two DANS molecules are displayed in the graphs of Fig. S2. As shown in Fig. S2, antiparallel linear DANS dimers are energetically unstable relative to the dissociation limit, being in contrast to the DANS dimers with a parallel linear alignment as well as those with antiparallel and parallel stacking alignments in Figure 4. This unstability in the antiparallel linear DANS dimers is due to repulsive interactions operated between positively charged NO_2 groups or between negatively charged $\text{N}(\text{CH}_3)_2$ groups. Thus, we concentrate our attention into energetically stable DANS dimers with a parallel linear alignment as well as those with antiparallel and parallel stacking alignments in the main text.

(a) Linear alignment
antiparallel fashion where NCH₃ groups are facing



(b) Linear alignment
antiparallel fashion where NO₂ groups are facing

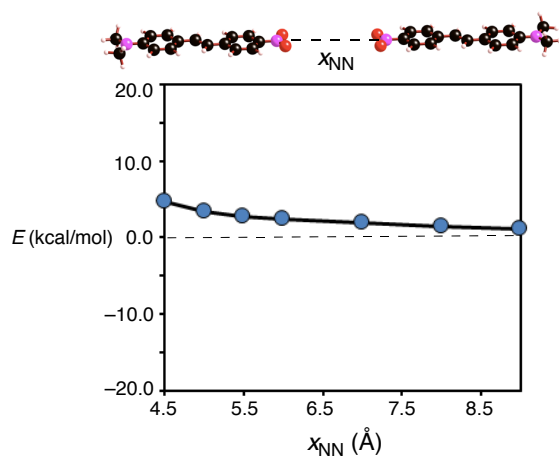


Fig. S2 Total energy changes of a linear DANs dimer in an antiparallel fashion constructed by changing the nearest nitrogen atoms of adjacent molecules (x_{NN}). Two types of the linear DANs dimer were considered: (a) one dimer has facing NCH₃ groups, and (b) the other is facing NO₂ groups. The total energies of shifted dimers relative to the dissociation energy toward two DANs molecules, obtained from B97D calculations, are displayed. The relative energies of the linear dimers are plotted as a function of x_{NN} .

S3. Intermolecular interactions in a stacking DANS dimer taken from $2 \times$ $\text{DANS}@ (m,m)$

Intermolecular interactions in a stacking DANS assembly taken from $n \times \text{DANS}@ (m,m)$ were evaluated, following the equation S3.

$$E_{\text{interact}}(n \times \text{DANS}@ (m,m)) = E_{\text{total}}(\text{inner } n \times \text{DANS}) - n \times E_{\text{total}}(\text{DANS}) \quad (\text{S3})$$

where $E_{\text{total}}(\text{inner } n \times \text{DANS})$ is the total energy of $n \times \text{DANS}$ assembly taken from $n \times \text{DANS}@ (m,m)$, and $E_{\text{total}}(\text{DANS})$ is that of single DANS molecule. Table S3 lists intermolecular interactions in a stacking DANS dimer taken from $2 \times \text{DANS}@ (m,m)$ (Fig. 6). Negative and positive E_{interact} values indicate attractive and repulsive intermolecular interactions in a certain DANS dimer, respectively. From Table S3, we obtain information in the intermolecular interactions in inner stacking dimers:

- (i) Positive E_{interact} values in $2 \times \text{DANS}@ (7,7)$ indicate that repulsive interactions were operated between the DANS molecules.
- (ii) Negative and significant E_{interact} values in $2 \times \text{DANS}@ (8,8)$ indicate that attractive interactions were operated between the DANS molecules.
- (iii) Negative and less significant E_{interact} values in $2 \times \text{DANS}@ (9,9)$ indicate that attractive interactions were weakly operated between the DANS molecules.
- (iv) Nearly zero E_{interact} values in $2 \times \text{DANS}@ (10,10)$ indicate that negligible interactions were operated between the DANS molecules.

By using the same definition, we obtained intermolecular interactions of a linear DANS dimer taken from optimized $2 \times \text{DANS}@ (m,m)$ structures (Fig. 5), as listed in Table S3. From Table S3, we found negative and less significant E_{interact} values in the inner linear dimers, indicating operation of weakly attractive intermolecular interactions.

Table S3 Intermolecular interactions of a DANS dimer taken from the optimized $2 \times \text{DANS}@ (m,m)$ structures.^a Unit is in kcal/mol.

| (m,m) | (7,7) | (8,8) | (9,9) | (10,10) |
|-------------------------|--|-------|-------|---------|
| | parallel stacking alignment ^a | | | |
| E_{interact}^b | 15.5 | -9.6 | -1.2 | 1.7 |
| | antiparallel stacking alignment ^a | | | |
| E_{interact}^b | 10.5 | -17.0 | -6.0 | -0.9 |
| | linear alignment ^a | | | |
| E_{interact}^b | -4.0 | -4.0 | - | - |

^a optimized $2 \times \text{DANS}@ (m,m)$ structures in stacking dimers are displayed in Fig. 6, and those in linear dimers are displayed in Fig. 5.

^b E_{interact} (kcal/mol): Intermolecular interactions in a DANS dimer taken from the optimized $2 \times \text{DANS}@ (m,m)$ structures, defined in Eq. S3.

S4. Structures for 3×DANS@(10, 10)

With respect to trimer arrangements inside a nanotube, two types were considered: one is that three DANS molecules are arranged in a parallel fashion (parallel arrangement), and in the other arrangement, one DANS molecule flips from the parallel trimer arrangement (flipping arrangement). As a container for a DANS trimer, we considered only the (10,10) nanotube, because it can have space large enough to accommodate it. Fig. S4 displays optimized structures for 3×DANS@(10,10) with the different trimer arrangements. In the parallel trimer arrangement (Fig. S4(a)), two DANS molecules approach, whose shortest carbon contact is 3.73 Å, and the other separates by larger than 4.84 Å. Similarly, the flipping trimer arrangement (Fig. S4(b)) has two DANS molecules with different direction of dipole moment approach, whose shortest carbon contact is 3.77 Å. The E_{bind} values defined in Eq. 5 are listed in Table S4, that also include the magnitude of intermolecular interactions in the inner trimers, evaluated by Eq. S3. As shown in Table S4, negative E_{interact} values indicate that attractive intermolecular interactions operated between three DANS molecules inside the (10,10) tube. Table S4 also lists static hyperpolarizability (β_0 values) of DANS trimers taken from the optimized 3×DANS@(10,10) structures (Fig. S4).

Table S4 Key properties in the B97D optimized 3×DANS@(10,10) structures

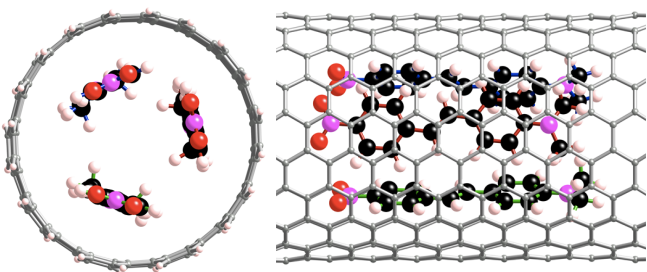
| Arrangement | parallel type | flipping type |
|-------------------------|---------------|---------------|
| E_{bind}^a | -173.0 | -179.3 |
| E_{interact}^b | -2.3 | -13.1 |
| $\beta_0/10^{-30}^c$ | 367 | 124 |

^a E_{bind} (kcal/mol): The energy value is defined in Eq. 5.

^b E_{interact} (kcal/mol): The magnitude of intermolecular interactions in inner trimers, defined in Eq. S3.

^c $\beta_0/10^{-30}$ (esu): Computed static hyperpolarizability in an inner DANS trimer.

(a) stacking alignment in a parallel fashion



(b) stacking alignment in a flipping fashion

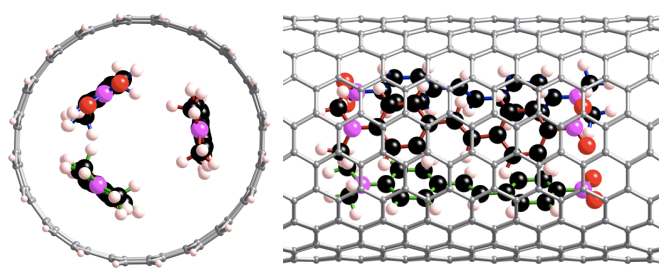


Fig. S4 Optimized structures for a DANs trimer in a stacking alignment inside the (10,10) nanotube ($3\times\text{DANS}@(\text{10,10})$). Two types of stacking alignment were considered: (a) a parallel type and (b) a flipping type where one molecule is flip from the parallel type. Nanotubes whose length is 2.2 nm were used.

S5. Shifting one DANS molecule from the original cofacial arrangement plays an important role in determining the intermolecular interactions.

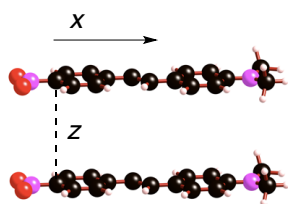
As shown in Fig. 6 and Table 4, DANS molecules in the stacking dimers within the (7,7) tube separate by ~ 3.0 Å. These separation ranges indicate that the two DANS molecules repulsively interact, according to Fig. 4. As shown in Table 4, another characteristic in $2 \times \text{DANS}@ (7,7)$ structures is that one DANS molecule shifts along the x -direction from the original cofacial stacking alignments in Chart 1. Here, we discuss intermolecular interactions of stacking DANS dimers constructed by shifting one DANS molecule from the original position (Chart 1) by x Å. In this situation, the intermolecular interactions are defined by the following equation,

$$E_{\text{interact}}(2 \times \text{DANS}(x)) = E_{\text{total}}(2 \times \text{DANS}(x)) - 2 \times E_{\text{total}}(\text{DANS}) \quad (\text{S5})$$

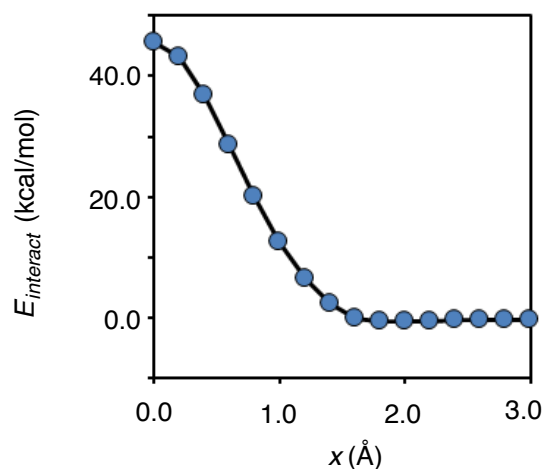
where $E_{\text{total}}(\text{DANS})$ and $E_{\text{total}}(2 \times \text{DANS}(x))$ are the total energy of the optimized structure for single DANS molecule, and that of a x Å-shifted DANS dimer. Fig. S5 displays $E_{\text{interact}}(2 \times \text{DANS}(x))$ values as a function of x , where positive $E_{\text{interact}}(2 \times \text{DANS}(x))$ values indicate operation of repulsive intermolecular interactions in a dimer structure.

First, let us discuss changes in the intermolecular interactions in parallel stacking DANS dimers whose interplane-separation (z) is fixed to 3.0 Å. Note that the original parallel dimer ($x = 0$ Å) has the positive $E_{\text{interact}}(2 \times \text{DANS}(x))$ value of 45.7 kcal/mol, indicating strong repulsive intermolecular interactions. As shown in Fig. S5a-i, their

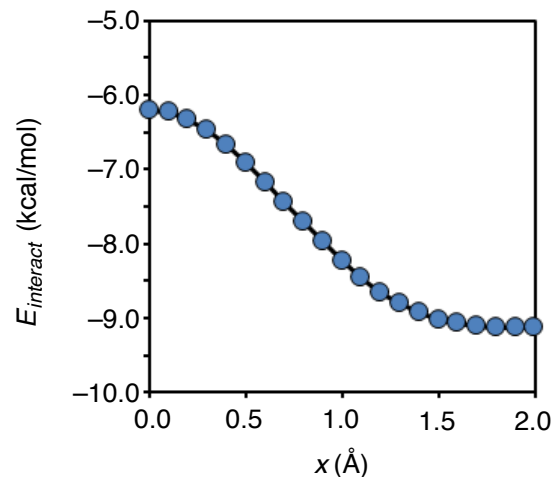
(a) Stacking alignment in a parallel fashion



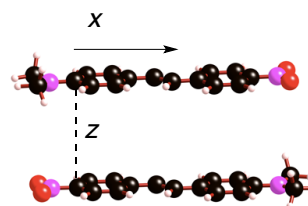
(i) $z = 3.0 \text{ \AA}$



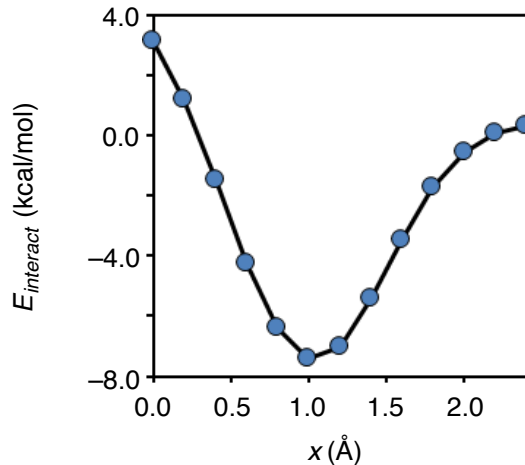
(ii) $z = 3.8 \text{ \AA}$



(b) Stacking alignment in an anti-parallel fashion



(i) $z = 3.0 \text{ \AA}$



(ii) $z = 3.5 \text{ \AA}$

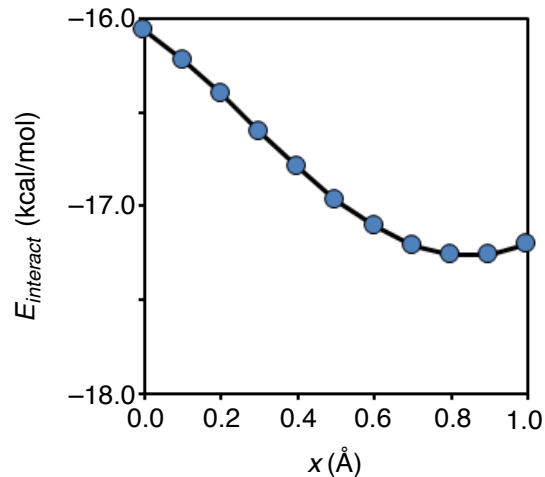


Fig. S5 Changes of the intermolecular interaction in a stacking DANS dimer constructed by shifting one molecule along the x -direction from an original arrangement in Chart 1. The interchain interactions, obtained from B97D calculations, are defined in Supporting Information 4. The x values indicate displacement of one molecule along the x -direction from the original cofacial arrangement. Two types of stacking alignment were considered; (a) parallel dimers with $z =$ (i) 3.0 and (ii) 3.8 \AA (b) antiparallel dimers with $z =$ (i) 3.0 and (ii) 3.5 \AA . Note that the z values correspond to separations between interplanes of DANS molecules contained in a dimer taken from the optimized $2 \times \text{DANS}@ (7,7)$ and $2 \times \text{DANS}@ (8,8)$ structures in Figure 6.

$E_{\text{interact}}(2 \times \text{DANS}(x))$ values sharply decrease, with an increase of x values. When x is larger than 1.8 Å, $E_{\text{interact}}(2 \times \text{DANS}(x))$ values become almost zero. These results indicate that strong repulsive interactions in the original stacking parallel dimer are reduced by shifting one DANS molecule along the x -direction. Similarly, repulsive interactions in the original antiparallel stacking dimer at $z = 3.0$ Å are diminished by increasing x values from 0 (Fig. S5b-i). At $x = 1.0$ Å the $E_{\text{interact}}(2 \times \text{DANS}(x))$ curve exhibits one minimum. The minimum is 7.4 kcal/mol stable relative to the dissociation limit toward two isolated molecules.

Similar analyses can be done to understand structural properties of stacking DANS dimers inside the (8,8) nanotube. Within the (8,8) nanotube, two DANS molecules in the parallel and antiparallel stacking alignments separate by ~ 3.7 and ~ 3.6 Å, respectively. Here, we constructed original stacking DANS dimers in parallel and antiparallel alignments (Chart 1) whose intermolecular separation (z) is 3.8 and 3.5 Å, respectively. Then, the original stacking dimers have attractive intermolecular interactions, because the $E_{\text{interact}}(2 \times \text{DANS}(x))$ values for the original parallel and antiparallel alignments are -6.2 and -16.1 kcal/mol, respectively. Figs. S5a-ii and S5b-ii found that the $E_{\text{interact}}(2 \times \text{DANS}(x))$ values in the parallel and anti-parallel dimers commonly decrease gradually with an increase of x values. These results indicate that attractive intermolecular interactions in the parallel and antiparallel stacking DANS dimers enhance by shifting one DANS molecule along the x -direction from the original arrangements in Chart 1. The potential energy surfaces in Fig. S5 can help us to well explain the optimized $2 \times \text{DANS}@ (m,m)$ structures, where m is 7 and 8.

S6. Optimized geometries for DANS dimers inside a zigzag nanotube

To check whether our conclusion can be found in zigzag nanotubes or not, preliminary information on DANS dimers inside zigzag nanotubes was obtained. Here, we considered two types of H-atom terminated zigzag nanotube whose length is 39.4 Å: the (12,0) and (13,0) tubes whose diameters are 0.95 and 1.02 nm, respectively. Previous computational reports indicated that spin-polarized states of H-atom terminated zigzag nanotubes are energetically stable relative to their spin-unpolarized states.^{S1,S2} According to the previous reports, the H-atom terminated (12,0) and (13,0) nanotubes in triplet spin states were first optimized by the B97D/6-31G** level of theory. Note that their triplet states are more stable than the quintet states in energy.

By using the optimized structures for H-atom terminated ($m,0$) nanotubes ($m = 12$ or 13) in the triplet state, let us discuss stable structures of DANS dimers inside the zigzag nanotubes. For this purpose, unrestricted DFT calculations of $2 \times \text{DANS}@(\mathit{m},0)$, whose number of contained atoms are up to 592, are time-consuming. Due to limiting our computational resources, we employed a QM/MM ONIOM approach to optimize $2 \times \text{DANS}@(\mathit{m},0)$ structures. In the QM/MM calculations, the QM region consists of inner DANS dimers, and the MM region consists of an H-atom terminated ($m,0$) nanotube. As the QM method, the B97D functional together with the 6-31++G** basis set were used, and AMBER force field^{S3} was used as the MM method. During the QM/MM optimization of $2 \times \text{DANS}@(\mathit{m},0)$ structures, atom positions of DANS guests were fully relaxed, while those of the tube host were frozen to optimal positions of the pristine H-atom terminated tube. By using QM/MM optimized

structures of $2 \times \text{DANS}@(\text{m},0)$ structures, we performed single-point B97D calculations, where the 6-31++G** basis sets were used for DANS dimers and the 6-31G** basis sets were used for nanotubes. We checked the reliability of the above-mentioned computational procedures compared with full DFT calculations with the same basis sets, by using a short zigzag nanotube (24.3 Å in length) containing one DANS molecule, as shown in Figure S6(a). As a result, we found that the procedures can yield results similar to full B97D-results, because the total energy obtained from the computational procedure is only 3.1 kcal/mol larger than that obtained from the full DFT B97D computation.

Figures S6(b) and S6(c) display QM/MM optimized $2 \times \text{DANS}@(\text{m},0)$ structures, where m is 12 and 13, respectively. Similar to the main text, three types of dimer alignments were considered in each zigzag tube: linear, and antiparallel- and parallel-stacking alignments. Obtaining their total energies from the B97D-single point calculations of the QM/MM optimized structures, we can determine which dimer structures are energetically stable in $2 \times \text{DANS}@(\text{m},0)$ structures, and their relative energies given in Figures S6(b) and S6(c). As shown in Figures S6(b), the linear DANS dimer inside the (12,0) tube is ~40 kcal/mol stable relative to the inner parallel and antiparallel stacking dimers. The unstability of inner stacking dimers would be due to strong repulsive interactions between DANS molecules as well as deformation of DANS molecules. These energy differences between the inner dimers inside the (12,0) tube are similar to those in the armchair (7,7) tube whose diameter is 0.95 nm. The results indicated selective formation of the linear DANS dimer inside the achiral tubes

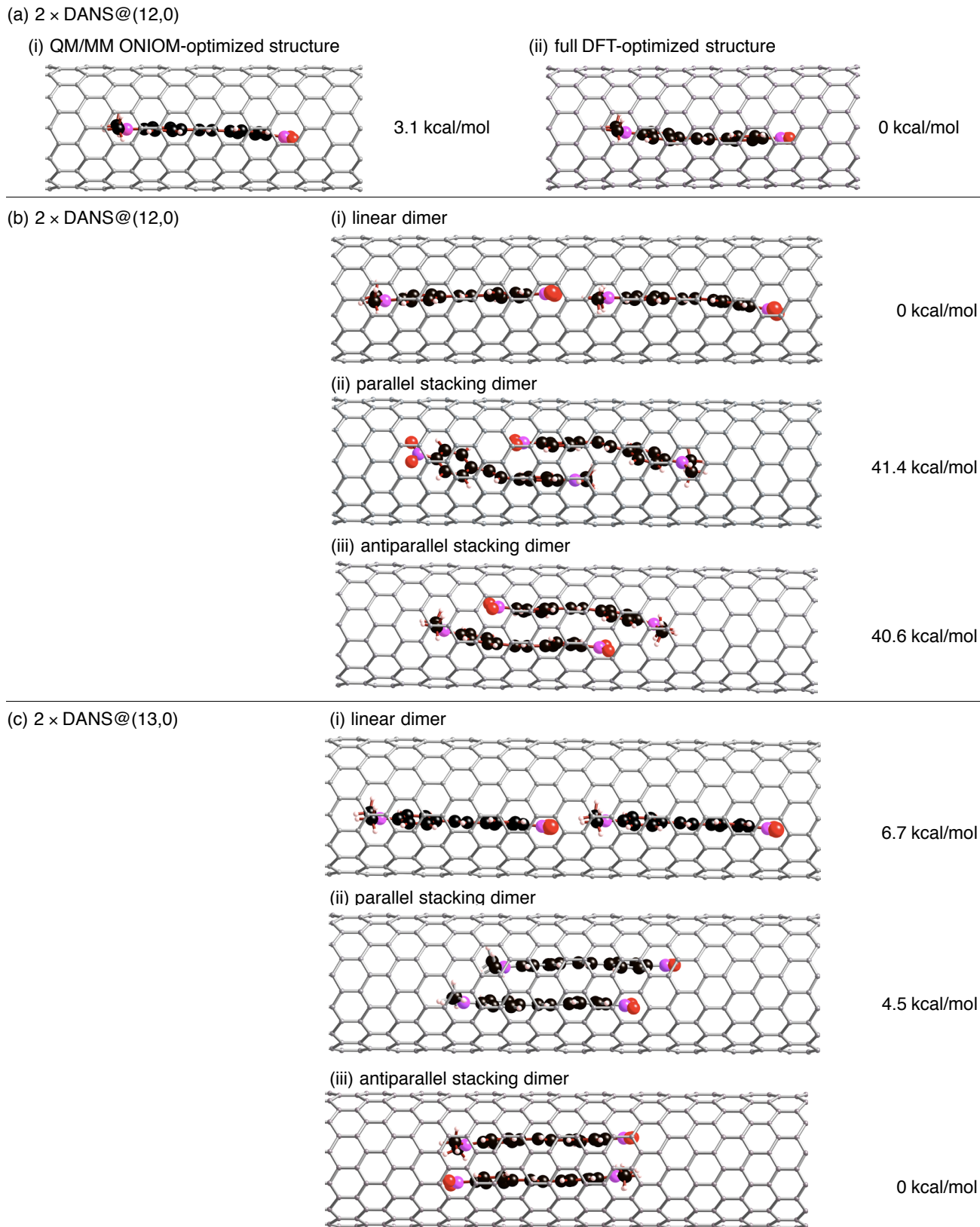


Fig. S6 Optimized structures for DANS molecules inside a zigzag nanotube. (a) a short (12,0) zigzag nanotube (24.3 Å in length) was used for the optimization of inner single DANS molecule by (i) a QM/MM approach and (ii) full B97D DFT computation. (b) a long (12,0) zigzag nanotube (39.4 Å in length) was used for the optimization of inner DANS dimers by a QM/MM approach. (c) a long (13,0) zigzag nanotube (39.4 Å in length) was used for the optimization of inner DANS dimers by a QM/MM approach. In (b) and (c), three types of dimer alignment were considered: (i) linear dimer, (ii) parallel stacking dimer and (iii) antiparallel stacking dimer. Their relative energies were obtained from single point B97D calculations by using the QM/MM optimized structures.

whose diameters are less than 1 nm. In contrast, we found that the three types of dimer alignment inside the (13,0) tube are energetically comparable, indicating that the nanotube whose diameter is larger than 1 nm allows DANS molecules to align in a stacking and linear fashion. Therefore, a threshold zigzag tube diameter for containing DANS molecules in linear or stacking alignments was found to be approximately 1.0 nm. The preliminary investigations found similar conclusions between the zigzag and armchair nanotubes in terms of stable DANS structures inside a nanotube. The similarity indicated important roles of tube diameter in determining structures of DANS guests. However, further investigation by using full DFT calculations should be needed to confirm whether our conclusion can be seen in other nanotubes including zigzag nanotubes.

(S1) A. J. Du, Y. Chen, G. Q. Lu, and S. C. Smith, *Appl. Phys. Lett.*, 2008, **93**, 073101.

(S2) J. Wu, and F. Hagelberg, *Phys. Rev. B*, 2009, **79**, 115436.

(S3) W. D. Cornell, P. Cieplak, C. I. Bayly, I. R. Gould, K. M. Merz, Jr., D. M. Ferguson, D. C. Spellmeyer, T. Fox, J. W. Caldwell, and P. A. Kollman, *J. Am. Chem. Soc.*, 1995, **117**, 5179–5197.